

13 Mar 1991, 1:30 pm - 3:30 pm

Experimental Studies on an Embedded Structure-Soil Interaction

Yuji Miyamoto

Kajima Corporation, Tokyo, Japan

Yasuhiro Ohtsuka

Kajima Corporation, Tokyo, Japan

Atsunobu Fukuoka

Kajima Corporation, Tokyo, Japan

Toshiaki Nasuda

Nuclear Power Engineering Test Center, Tokyo, Japan

Masanori Izumi

Tohoku University, Miyagi, Japan

Follow this and additional works at: <https://scholarsmine.mst.edu/icrageesd>



Part of the [Geotechnical Engineering Commons](#)

Recommended Citation

Miyamoto, Yuji; Ohtsuka, Yasuhiro; Fukuoka, Atsunobu; Nasuda, Toshiaki; and Izumi, Masanori, "Experimental Studies on an Embedded Structure-Soil Interaction" (1991). *International Conferences on Recent Advances in Geotechnical Earthquake Engineering and Soil Dynamics*. 19.

<https://scholarsmine.mst.edu/icrageesd/02icrageesd/session05/19>

This Article - Conference proceedings is brought to you for free and open access by Scholars' Mine. It has been accepted for inclusion in International Conferences on Recent Advances in Geotechnical Earthquake Engineering and Soil Dynamics by an authorized administrator of Scholars' Mine. This work is protected by U. S. Copyright Law. Unauthorized use including reproduction for redistribution requires the permission of the copyright holder. For more information, please contact scholarsmine@mst.edu.

Experimental Studies on an Embedded Structure-Soil Interaction

Yuji Miyamoto, Yasuhiro Ohtsuka and Atsunobu Fukuoka
 Research Engineer, Kajima Corporation, Tokyo, Japan

Toshiaki Nasuda
 Section Manager, Nuclear Power Engineering Test Center, Tokyo, Japan

Masanori Izumi
 Professor of Civil Engineering, Tohoku University, Miyagi, Japan

SYNOPSIS: This paper describes the results of experimental studies performed for evaluation of the embedment effects on the dynamic characteristics of the structure and the correlation analyses between the test results and the calculated results.

The vibration tests of large scale models constructed on actual soil are carried out with the purpose of obtaining the basic data for verification study on analysis codes. In the correlation analyses, the methods used here are the sway-rocking model and the axisymmetric finite element method. These methods are confirmed to be applicable to analyse the response of the embedded structures.

INTRODUCTION

The soil-structure interaction effects have an important role on the dynamic characteristics of very massive and stiff structure during earthquakes. The backfill and the surrounding soil have a significant effect on soil-structure interaction of the embedded structure.

In this study, large scale models are constructed on actual soil and experimental studies are carried out for evaluation of the embedment effect on the structure response. The forced vibration tests of the models are performed with the conditions of different embedment depths. The responses of the model are measured and the dynamic soil impedance functions are evaluated. Furthermore, the response properties of the backfill soil, the surrounding soil and the earth pressure at the foundation bottom and the side wall of the embedded foundation are obtained. In the correlation analyses, the following two analytical methods are used: (1) S-R Model employing the soil impedances of the bottom determined by the three dimensional wave propagation theory in layered soil and the side impedances calculated by Novak's method, and (2) Axisymmetric Finite Element Method.

CONDITIONS OF EXPERIMENT

1. Test Model

The general view of the test model is shown in Photo.1. The test model was scaled down to 1/10 in consideration of the fundamental vibration characteristics (non-dimensional frequency, weight ratio of each part and sway/rocking ratio, etc.) of a BWR-type reactor building in Japan. The cross section of the model is shown in Fig. 1. The model is a 3-story RC structure with a 8mx8m square foundation. The basement part of which weight is about 450 ton, was constructed after excavating the ground to 5m depth. The forced vibration tests were carried out under the condition of different embedment depth (A1, A2 and A3 tests). Fig. 2 illustrates

the test conditions of backfill soil and test model. Next, the super-structure was constructed, and the forced vibration test of 5m embedment depth (A4 test) was conducted. The total weight of A4 test model was about 657 ton.

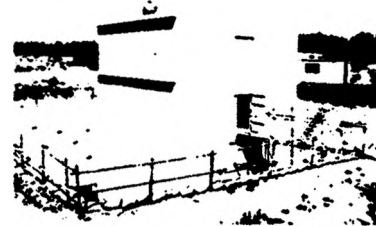


Photo.1 Test Model

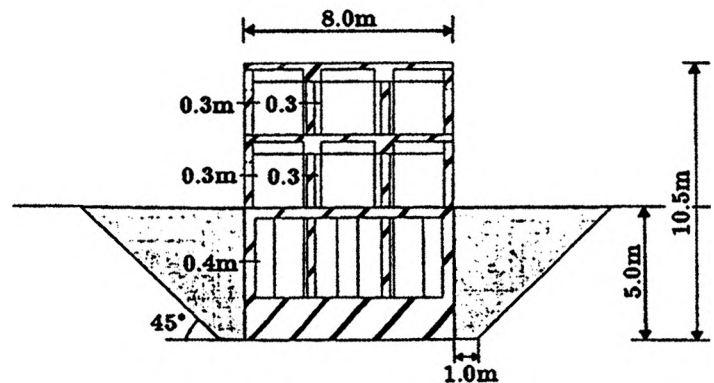


Fig. 1 Cross Section of Test Model (A4 Test)

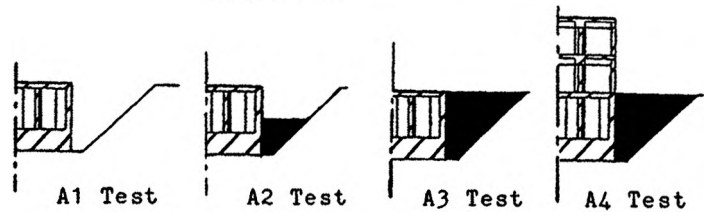


Fig. 2 Test Conditions

2. Soil Condition

The test model was constructed on an existing soil. According to the boring survey and the PS logging, the test site was confirmed to be layered half space. At the layer under the foundation bottom, shear wave velocity is 300m/s-425m/s, and at the layer which is more than 7m under the foundation bottom, shear wave velocity is greater than 1350m/s. From the elastic wave survey of the ground surface after excavation, a soft zone was found near the surface of excavated ground. Backfill soil was controlled by compacting every 15cm thickness to be the same condition of shear wave velocity and density of each layer. At the time of A3 test (5m embedment depth), shear wave velocity of the backfill soil was 130m/s near the surface and about 160m/s around the foundation bottom. This can be considered as the effect of overburden pressure. This result agrees well with the dynamic simple shear test when considering overburden pressure of backfill soil in the laboratory.

3. Measuring System

The responses of the test model were measured by displacement transducers. The responses of backfill and surrounding soil were also measured by accelerometers and displacement transducers. The earth pressures at the bottom of the foundation and the side walls were obtained by earth-pressure gauges. The strain of backfill soil was observed by dynamic strain gauges. The number of measuring components of A4 test totaled 126.

4. Method of Experiment

The forced vibration tests were performed by applying sinusoidal excitation which was generated by an exciter installed in the basement (A1, A2 and A3 tests) or on the super-structure (A4 test). The forces were applied in NS, EW (horizontal) and UD (vertical) direction for A1 test, and NS, UD directions for A2 and A3 tests. For A4 test, the excitations were executed in two horizontal directions. As for the excitation force, small force levels were kept for each step so that the backfill and the surrounding soil remained in elastic range.

TEST RESULTS

1. Response of Test Model

The natural frequencies, damping factors and displacement ratios are summarized in Table I. Resonance curves and phase lag curves of A1, A2 and A3 tests in the NS excitation are plotted in Fig. 3. This figure shows the displacement of foundation bottom derived from the measured value. As shown in TABLE I and Fig. 3, the decrease of amplitude and increase of natural frequency and radiation damping are confirmed in accordance with increasing embedment depth. Fig. 4 shows the vibration mode of the test model around the natural frequency (A1, A3 tests). The basement part of the test model vibrates as a rigid body. At the time of A1 test, UD components of NE and SW corner is larger than those of NW and SE corner which is probably caused by the irregularity of the soil under the foundation bottom. However, at the time of A3 test, the differences of these amplitude become small due to the effect of backfill soil.

Fig. 5 shows the ratio of the horizontal displacement at the foundation bottom to that at the top of basement part. Around the natural frequency, the displacement ratios at A1, A2 and A3 tests are similar, however, these values change significantly depending on the frequency. The resonance curves and phase lag curves of A3 and A4 tests in the NS excitation are shown in Fig. 6. On A3 test, resonance peak did not clear. For A4 test, however, the increase of the response is remarkable due to the effect of the super-structure inertia. Fig. 7 shows the ratio of the horizontal displacement at the foundation bottom to that of the top of basement part in the case of A3 and A4 tests. Dynamic characteristics of displacement ratio are similar for A3 and A4 tests. But on A4 test, it can be found that rocking ratio increases in the lower frequency range.

TABLE I. Test Results

Test	Direction of Force	Natural Frequency (Hz)	Damping Factor (%)	Displacement Ratio (%)		
				Sway	Rocking	Super-Structure
A1	NS	10.1	7.6	37	63	--
	EW	10.1	8.3	38	62	--
	UD	15.8	6.2	--	--	--
A2	NS	11.7	8.5	41	59	--
	UD	15.4	9.3	--	--	--
A3	NS	14.3	41.7	38	62	--
	UD	17.2	33.9	--	--	--
A4	NS	8.9	14.7	14	76	10
	EW	8.8	17.0	19	69	12

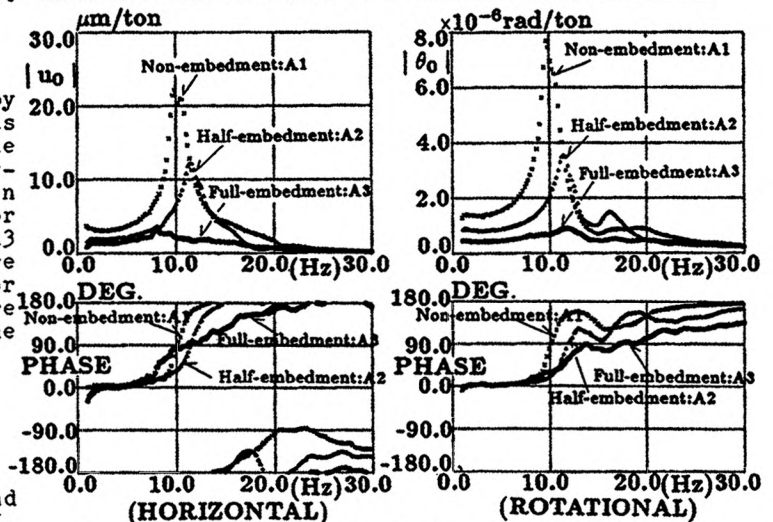


Fig. 3 Comparison of Displacement Resonance and Phase Lag Curves at Foundation Bottom

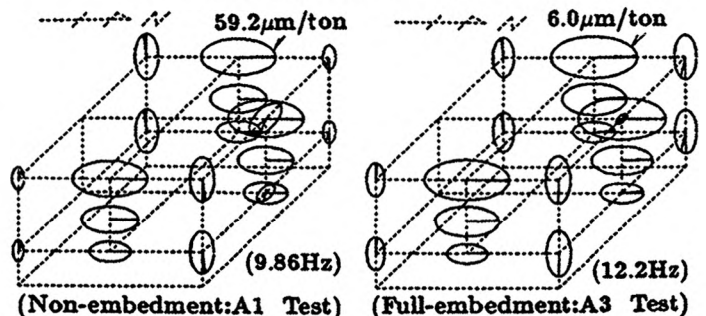


Fig. 4 Vibration Modes of Test Model near Natural Frequency

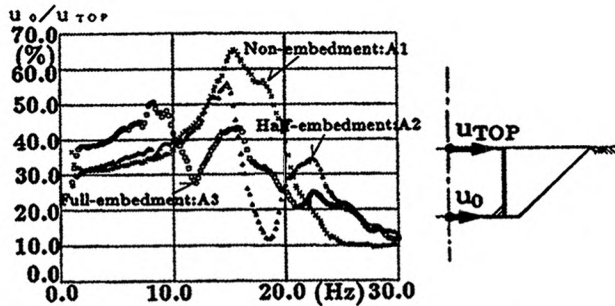


Fig. 5 Comparison of Horizontal Displacement Ratios of u_0 to u_{top} at Basement Part

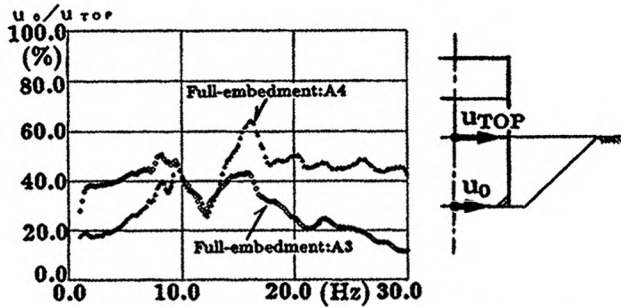


Fig. 7 Comparison of Horizontal Displacement Ratios of u_0 to u_{top} at Basement Part (A3 and A4 Tests)

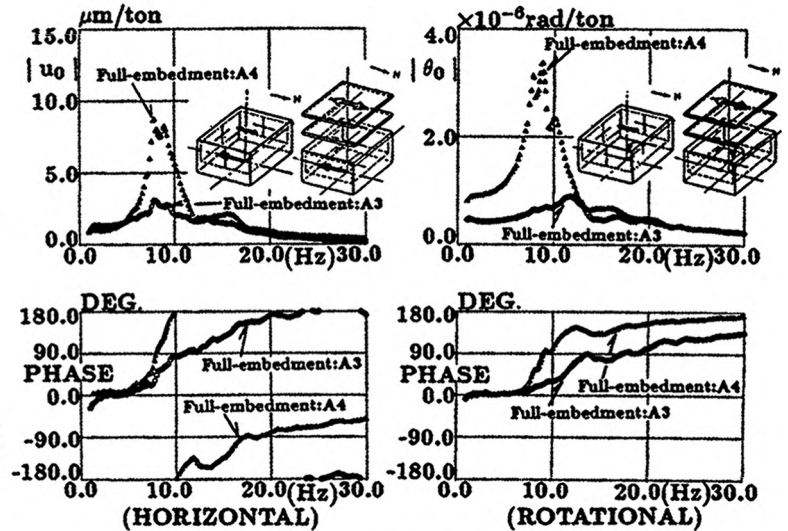


Fig. 6 Comparison of Displacement Resonance and Phase Lag Curves at Foundation Bottom between A3 and A4 Tests

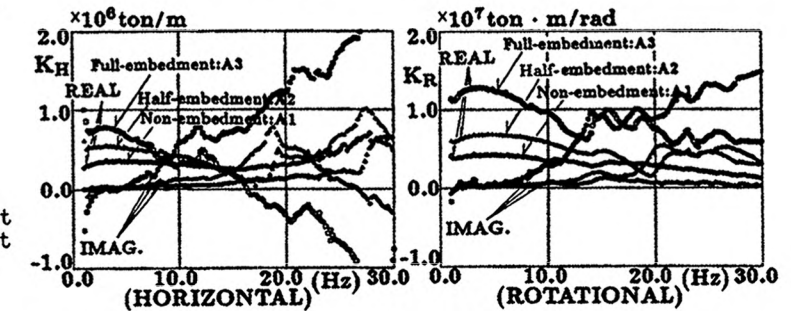


Fig. 8 Comparison of Combined Soil Impedances obtained by Test Results of Foundation Model

2. Soil Impedances

In this study, combined soil impedances, which are expressed by equations (1), are derived from test results.

$$Q/u_0 = K_H = K_{HH} + K_{HR} \cdot \theta_0/u_0$$

$$M/\theta_0 = K_R = K_{RR} + K_{RH} \cdot u_0/\theta_0$$

where

u_0, θ_0 : Horizontal and Rotational displacements at Foundation Bottom (Test Results)

Q, M : Shearing force and Moment at Foundation Bottom

K_H, K_R : Combined Horizontal and Rotational Impedances

K_{HH}, K_{RR} : Dynamic Horizontal and Rotational Impedances

$K_{HR} = K_{RH}$: Dynamic Coupling Impedances

Fig.8 shows the combined soil impedances for A1, A2 and A3 tests in the NS excitation. The embedment effect on the soil impedances is to increase the real and imaginary parts in accordance with increasing embedment depth and complicates the dynamic properties. Fig.9 shows the combined soil impedances of A4 test compared with that of A3 test in the NS excitation. These combined soil impedances do not coincide mutually, because the contribution of coupling to the combined soil impedances is different for each test. But, the dynamic characteristics are similar due to the influence of the backfill and surrounding soil.

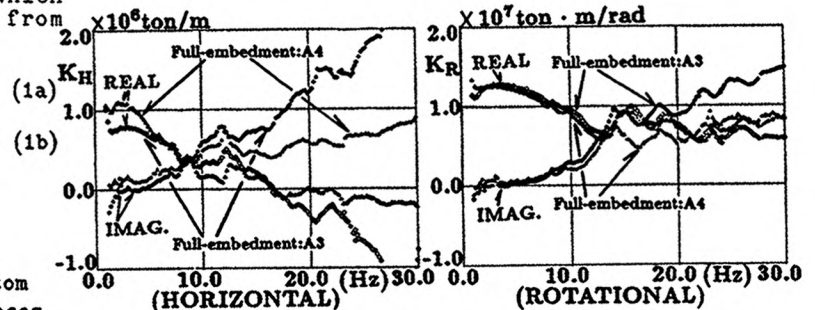


Fig. 9 Comparison of Combined Soil Impedances between A3 and A4 Tests

3. Earth Pressure

Fig.10 shows the static earth pressure distribution for A1 and A3 tests. The average value of the measured pressure is 623 g/cm^2 for A1 test and 696 g/cm^2 for A3 test. Assuming uniform distribution and considering the weight of test model, the bottom pressure should be about 700 g/cm^2 . The earth pressure distribution at the foundation bottom hardly changes because of the embedment effect. For the side pressure, it is the largest at the middle of the embedment depth. Fig.11 shows the dynamic earth pressures distribution for A1 and A3 tests near

natural frequency. The bottom pressure distribution seems to be the distribution of rigid plate. The side pressure distribution indicates a larger amplitude in the vicinity of the ground surface, corresponding with a rotational motion of the test model.

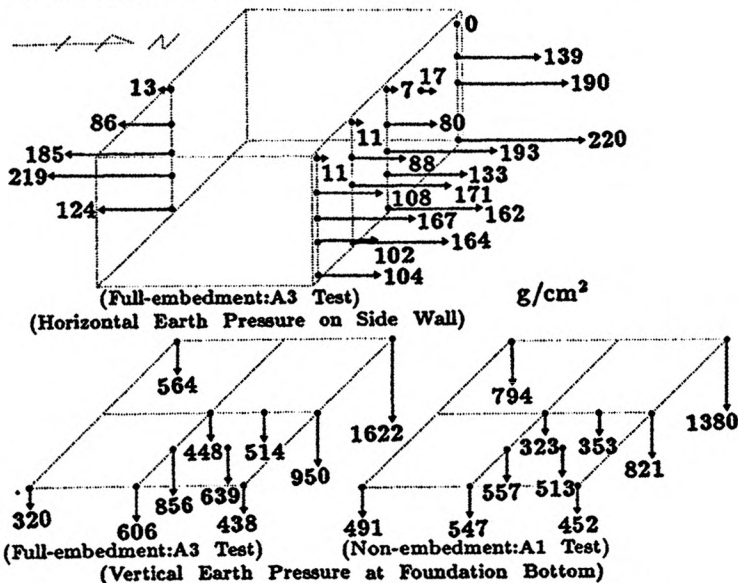


Fig.10 Comparison of Static Earth Pressure Distribution between A1 and A3 Tests

CORRELATION ANALYSES

Many methods have been proposed for the analyses of the dynamic characteristics of embedded structure. This paper describes the comparative investigations of the forced vibration test results in the NS excitation by the following two analytical techniques.

1. Analysis Models

In the correlation analyses, the (embedded) basement part is treated as a rigid body based on the measuring mode of the basement (Fig. 4) and the test structure is assumed as a multi-lumped mass model with bending and shearing deformation. For the evaluation of dynamic soil impedances, the following two analytical techniques are used: (1) Sway-Rocking model, hereafter called "S-R" model, the soil impedances K_{HH} (horizontal impedance), K_{RR} (rotational impedance) and K_{HR} (coupling impedance) at the foundation bottom and the soil impedances K_u (horizontal impedance) and K_ϕ (rotational impedance) at the side wall of the embedded basement part are calculated independently. The bottom impedances are defined assuming that the base level is the ground surface, and calculation is executed using the three dimensional wave propagation theory, while Novak's method is applied for the calculation of the side impedances. The side impedances K_s (shear impedance), which represent shear resistance of backfill and surrounding soil in accordance with rotation of the test structure, are added in the sway-rocking model, hereafter called "S-R with K_s " model. The resulting S-R model is shown in Fig.12. And, (2) Axisymmetric Finite Element Method, hereafter called "FEM" model, the energy dissipation from the analysis boundary of the finite soil towards the outside is evaluated

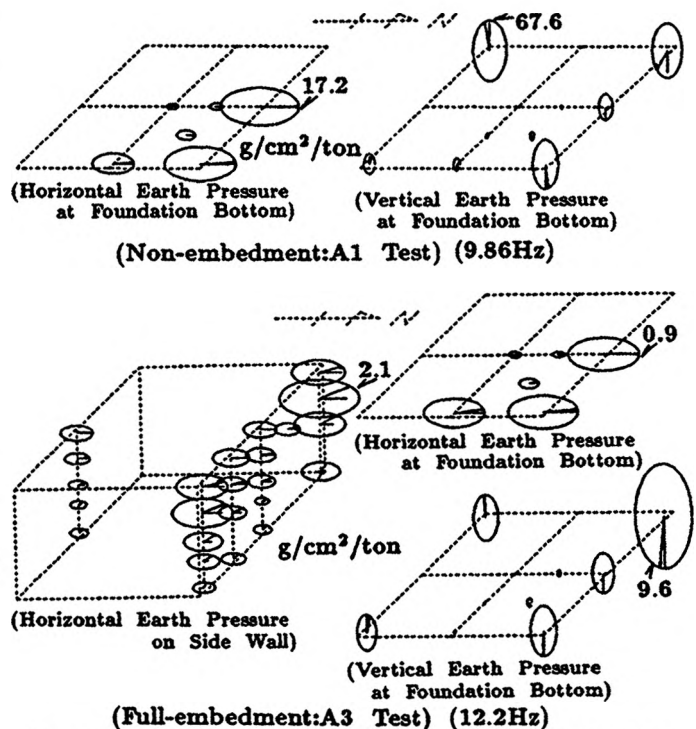


Fig.11 Comparison of Dynamic Earth Pressure Distribution between A1 and A3 Tests

with addition of viscous damping at the bottom boundary and transmitting boundary at the side boundary. The FEM model is shown in Fig.13. The constants of the soil property adopted in this correlation analysis are tabulated in TABLE II. These values are determined based on the measured data of the PS logging and the exploration with elastic waves of the test site. Fig.14 shows soil models of the foundation bottom in the case of A1 test (non-embedment).

TABLE II. Soil Constants for Analysis

(a) Sway-Rocking Model

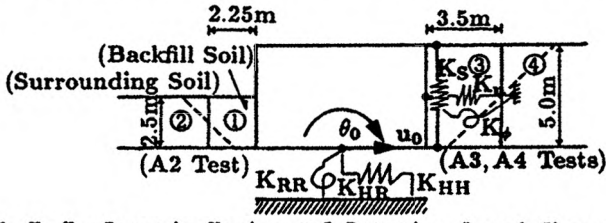
	Mass Density ρ (t/m ³)	Shear Wave Velocity V_s (m/s)	Poisson's Ratio ν	Damping Factor h (%)
①	1.8	130	0.30	2
②	1.7	285	0.35	5
③	1.8	150	0.30	2
④	1.7	285	0.35	5

(b) Axisymmetric FEM Model

	Mass Density ρ (t/m ³)	Shear Wave Velocity V_s (m/s)	Poisson's Ratio ν	Damping Factor h (%)
①	1.5	140	0.39	5
②	1.7	270	0.29	5
③	1.7	340	0.34	5
④	1.7	400	0.12	3
⑤	1.7	400	0.46	3
⑥	1.9	1330	0.11	3
⑦	2.1	1600	0.35	3
⑧	1.7	230	0.12	5
⑨	1.8	110	0.30	2
⑩	1.7~1.8	110~150	0.30	2~4

The figure (a) shows the S-R model and the figure (c) shows the FEM model, the Axisymmetric

FEM model, in Fig.13. The figure (b) shows the Axisymmetric FEM model without the surrounding soil represented by dotted line.



K_u, K_ϕ, K_s : Dynamic Horizontal, Rotational and Shear Impedances

* K_{HH} , K_{RR} and K_{HR} are calculated using the equivalent layered soil model to axisymmetric FEM model (Shear wave velocity is equal to 250m/s and Poisson's ratio is 0.12 for the soil property of the corresponding constants number ③ and ④ in Fig.13).

Fig.12 Sway-Rocking Model

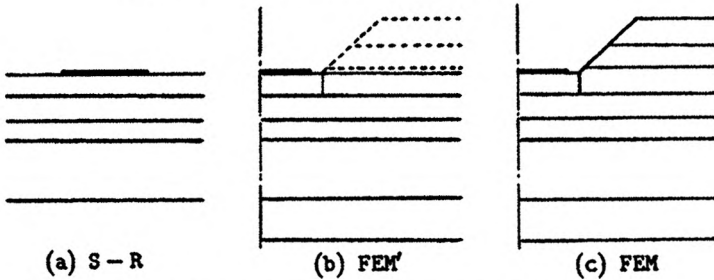


Fig.14 Soil Model at Foundation Bottom (Embedment depth is equal to 0m)

2. Soil Impedances

Fig.15 shows the comparison of dynamic impedances between S-R and FEM model in the case of A1 test (non-embedment). As for the horizontal springs K_{HH} , the discrepancies between S-R and FEM' model caused by soft soil under the foundation bottom become significant with the frequency range over 10Hz. The differences between FEM' and FEM caused by surrounding soil are recognized in the frequency range over 6Hz and become more significant with the higher frequency range. As for the rotational springs K_{RR} , three analysis results are mutually similar except for the few differences in the higher frequency range.

Fig.16 shows the comparison of combined soil impedances calculated by eqs.(1). In the case of A1 test, the real and imaginary part of K_H by FEM model show good agreement with the test results in the lower frequency range, while the real part is underestimated by S-R model. The discrepancies between S-R model (or FEM') and FEM model become significant with the higher frequency range due to the influences of surrounding soil. As for K_R , the two analyses model results show good agreement with the test results. The influence of coupling impedances can not be neglected in the case of non-embedment from the comparison of dynamic soil impedances between Fig.15 and Fig.16(a). In the case of A2 test (half-embedment), the analytical results conform well to the test results, while the real part is somewhat underestimated in the lower frequency range, and the imaginary part by S-R model is overestimated. In the case of A3 test (full-embedment), the analytical results by

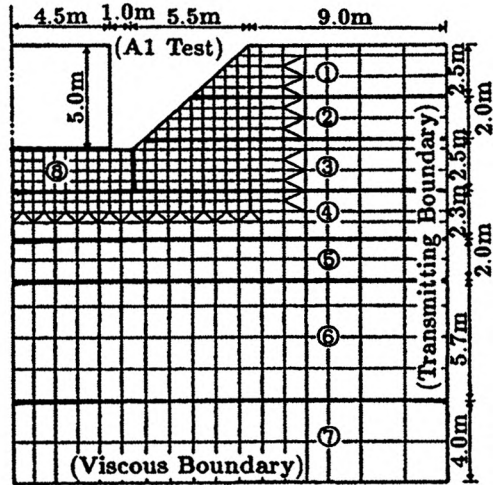
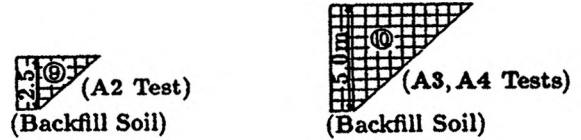


Fig.13 Axisymmetric FEM Model

FEM show good agreement with the test results, while the differences between the result by S-R model and the test result are similar in the frequency characteristics to the case of A2 test. As for the real part of K_R , the result by S-R with K_s model increases, while the imaginary part is invariable. As shown in Fig.16(d), the analytical results by FEM conform well with the A4 test results except for few discrepancies in the higher frequency range, while similar differences in the case of A3 test are recognized between the result by S-R model and the A4 test result.

Fig.17 shows the comparison of ratios of the rotational displacement to the horizontal displacement at the foundation bottom in the cases of A3 and A4 tests. As shown in Fig.16 and Fig.17, the discrepancies between the combined soil impedances of A3 and A4 tests arise from the frequency characteristics of ratios of the rotational displacement to the horizontal displacement.

Fig.18 shows the comparison of the dynamic soil impedances with 5m embedment depth. In this figure, K_{HH} , $K_{HR}(=K_{RH})$ and K_{RR} in eqs.(1) are evaluated using the data of A3 and A4 tests, (K_H, K_R, u_0 and θ_0), by the method of least squares. As shown in Fig.18, the analytical results by S-R model conform approximately with the test results, while the real part is underestimated and the imaginary part is overestimated in the lower frequency range. The analytical results by FEM model show good agreement with the test results, while the differences are recognized between the analytical results and the test results in the

higher frequency range. It is confirmed that the influence of the coupling impedance on the horizontal component of the combined soil

impedances is greater than the rotational component through Figs.15-17.

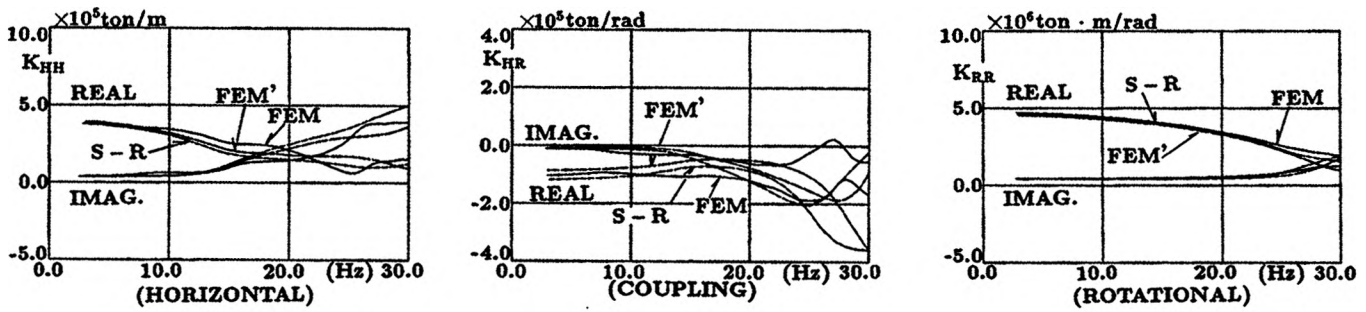


Fig.15 Comparison of Dynamic Soil Impedances (Embedment depth is equal to 0m)

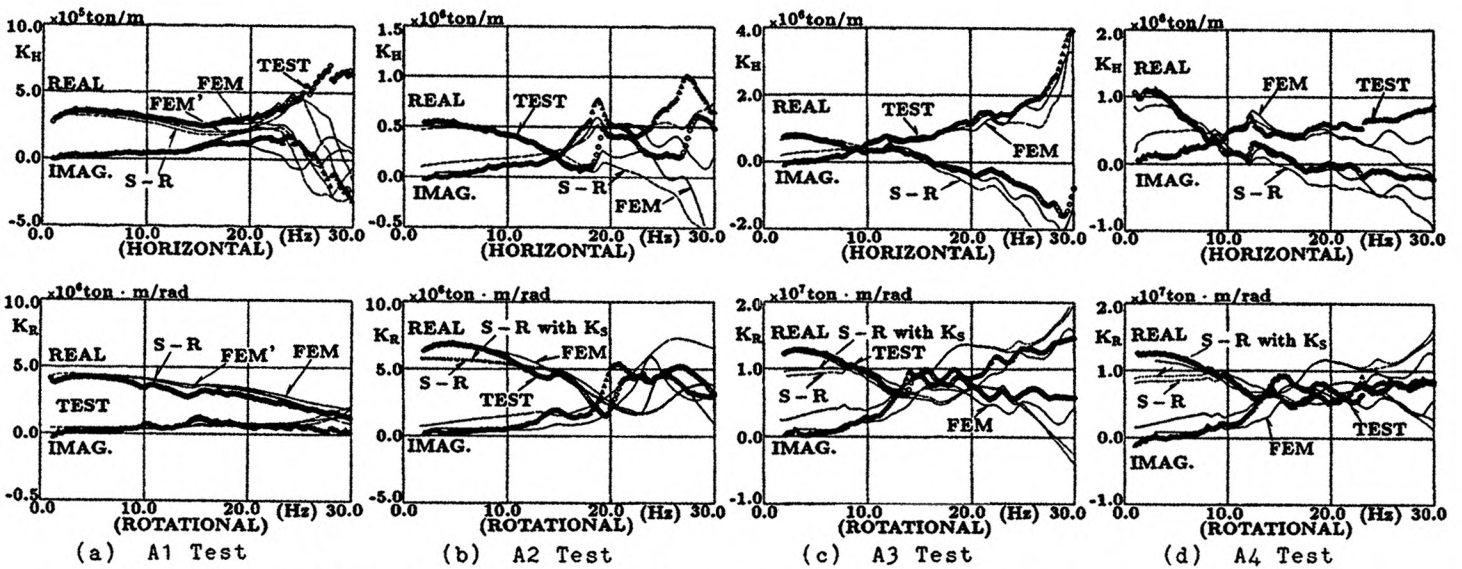


Fig.16 Comparison of Combined Soil Impedances between Tests and Analyses

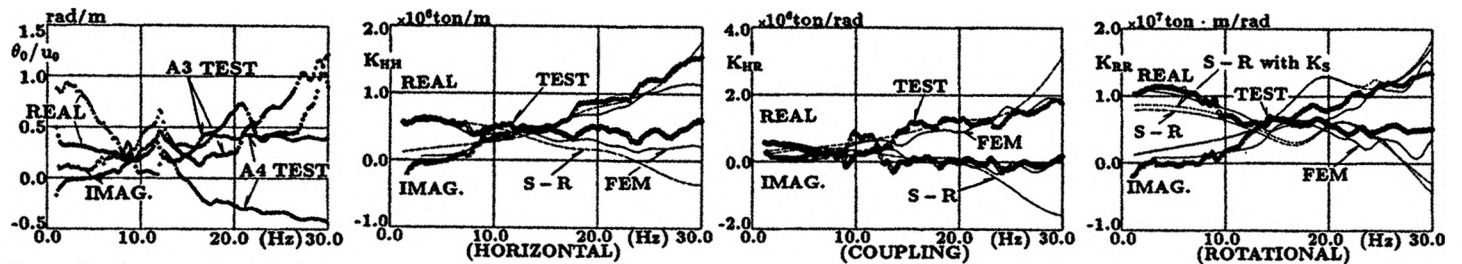


Fig.17 Comparison of Ratios of θ_0 to u_0 at Foundation Bottom (A3, A4 Tests)

Fig.18 Comparison of Dynamic Soil Impedances between Tests and Analyses (Embedment depth is equal to 5m)

3. Resonance Curves of Displacement

Fig.19 shows the comparison of the resonance curves at the foundation bottom used by the dynamic soil impedances K_{HH} , K_{HR} and K_{RR} . These test results show that the structure response amplitude decreases and the resonance frequency shifts to a higher frequency range. The frequency response characteristics due to the influence of the backfill and the surrounding

soil cause complication in accordance with increasing embedment depth. The analytical results by FEM model show good conformity with the test results. The discrepancies between the analytical results by S-R model and test results become more significant in accordance with increasing depth of backfill soil. The S-R with K_s model increases horizontal amplification, but its increment is small.

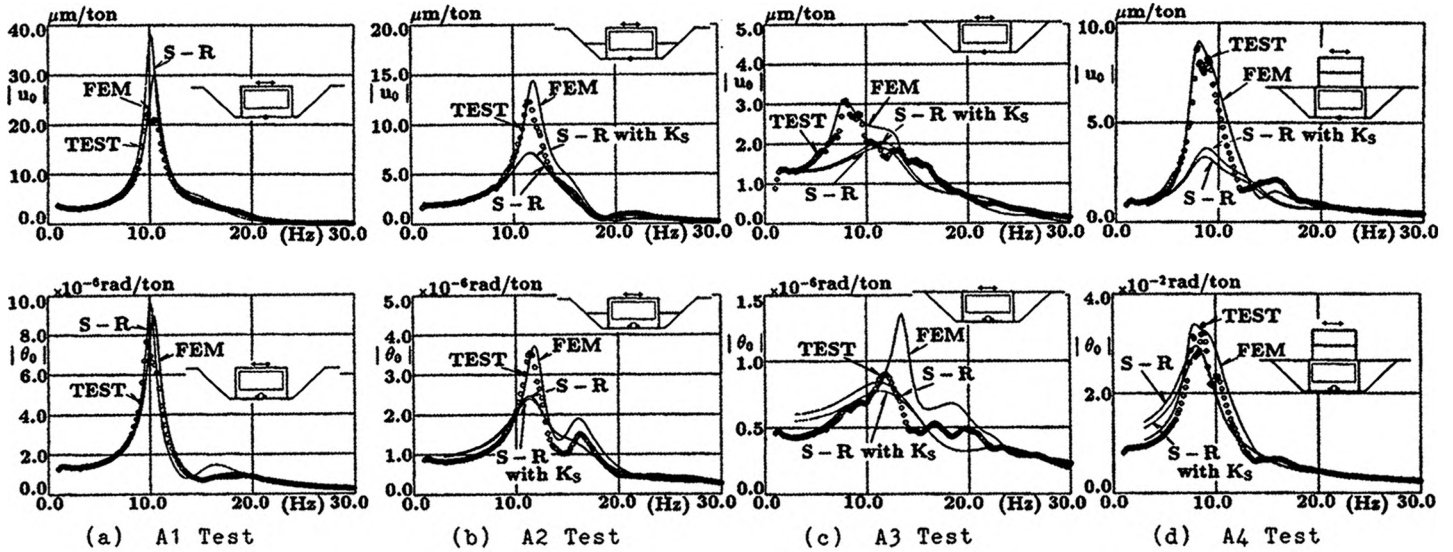


Fig.19 Comparison of Displacement Resonance Curves at Foundation bottom

4. Resonance Curves of Earth Pressure

Hereafter the analytical results by FEM model will be adopted only as a comparison model with the test results. Fig.20 shows the comparison of the resonance curves of vertical earth pressure at the foundation bottom in the horizontal excitation. These test results show that the vertical earth pressure is similar in the frequency response characteristic to the rotational displacement. The response amplitude increases at the border of the foundation bottom. The analytical results show good agreement with the test results, while the amplifications calculated by FEM are somewhat overestimated around the

first predominant frequency. Fig.21 shows the comparison of the resonance curves of earth pressure on the side wall of the embedment structure in the horizontal excitation. These test results conform well with the characteristics of the structure response and show that the increase of amplitudes is observed due to the inertia of the super-structure of A4 test. The analytical results show well the characteristics of the earth pressure obtained from the test results, while the amplifications by FEM model are overestimated along the horizontal axis.

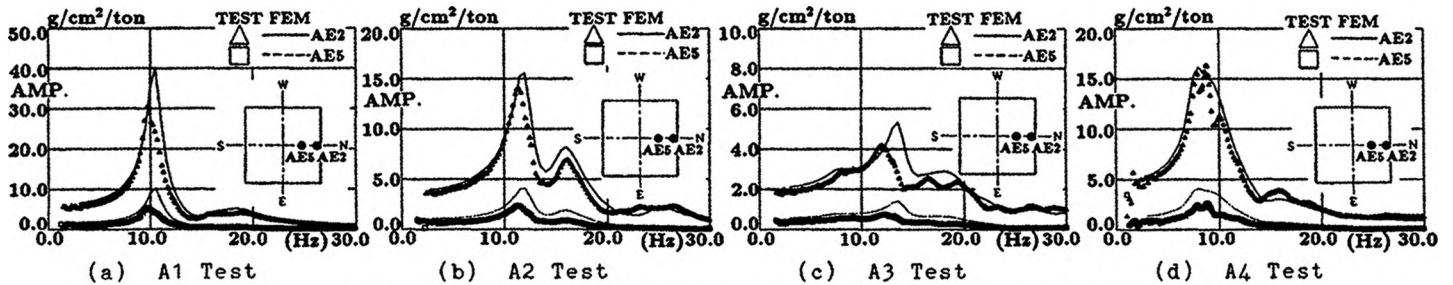


Fig.20 Comparison of Resonance Curves of Vertical Earth Pressure at Foundation Bottom

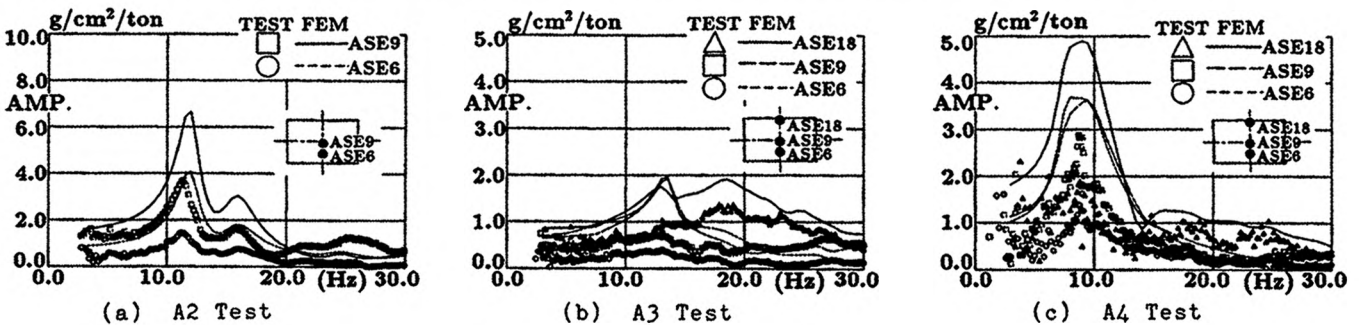


Fig.21 Comparison of Resonance Curves of Horizontal Earth Pressure on Embedment Side Wall

5. Resonance Curves of Acceleration

Fig.22 shows the comparison of resonance and phase lag curves of horizontal acceleration in the backfill and the surrounding soil. As shown in Fig.22, the analytical results are in good agreement with the test results, while there is some discrepancy in the higher frequency range. Fig.23 shows the comparison of acceleration ratios defined as accelerations on the ground

surface of backfill (or surrounding) soil divided by those at the bottom. The analytical results represent a tendency regarding that the acceleration ratios approximately correspond with the frequency response characteristics of dynamic soil impedances (Fig.18). Therefore it is confirmed that the dynamic soil impedances in Fig.18 are influenced by the dynamic properties of backfill and surrounding soil.

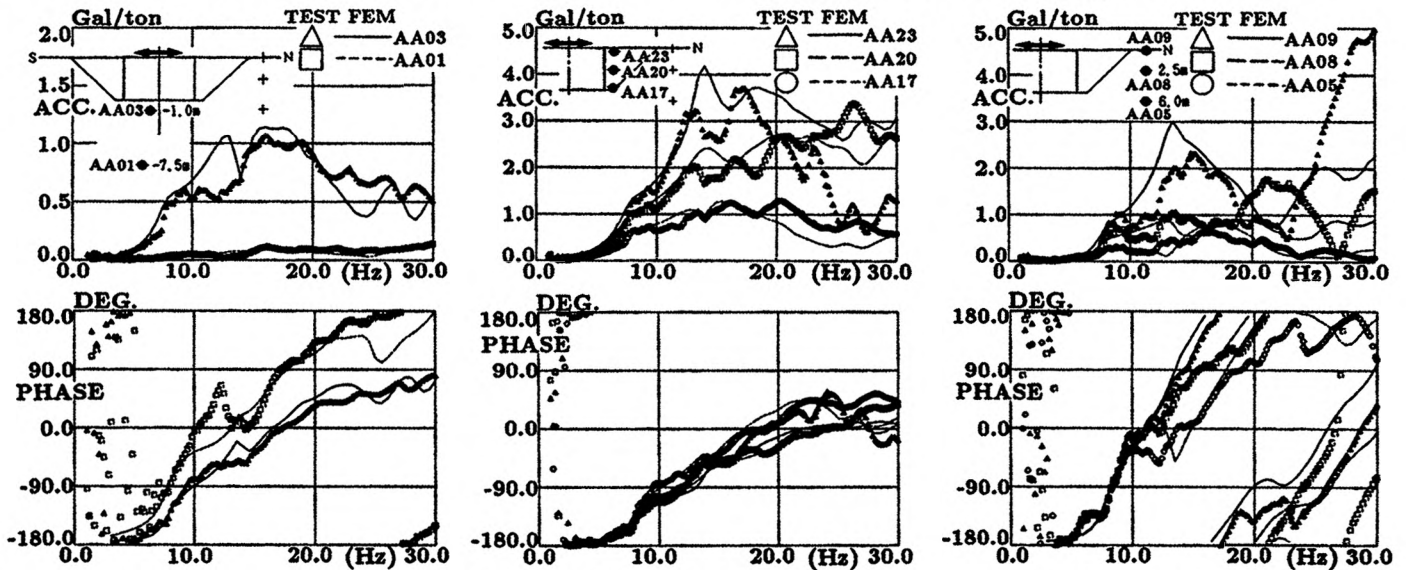


Fig.22 Comparison of Resonance and Phase Lag Curves of Horizontal Acceleration in Backfill and Surrounding Soil (A3 Test)

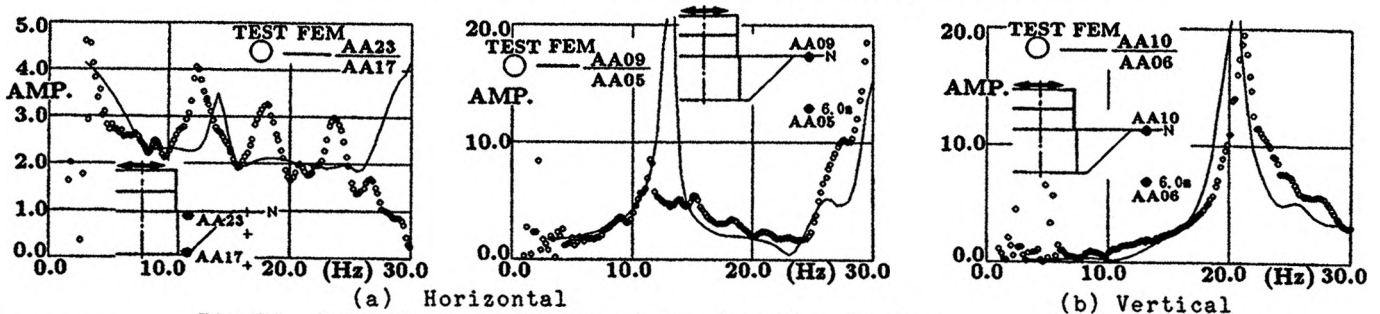


Fig.23 Comparison of Ratios of Acceleration in Backfill and Surrounding Soil

CONCLUSIONS

The concluding remarks obtained from the experimental and analytical studies are as follows:

1. The embedment effect on the soil impedances increases in accordance with increasing embedment depth and complicates the dynamic properties. The structure response amplitude decreases and the resonance frequency shifts towards high frequency.

2. The influence of coupling on the combined soil impedances can not be neglected in the case of non-embedment as is well known in the embedded case, and appears stronger on the horizontal components than the rotational components.

3. The response of the embedded structure depends on the dynamic characteristics of the backfill and the surrounding soil.

4. The earth pressure distribution at the

foundation bottom hardly changes due to the embedment effect. The side pressure distribution indicates larger amplifications in the vicinity of the ground surface, corresponding with a rotational motion of the test model.

5. The analysis methods used here, S-R model and Axisymmetric FEM model are confirmed to be valid for evaluating the response of embedded structures and the useful data are obtained to verify the rational analysis method.

ACKNOWLEDGEMENTS

This work was carried out as an entrusted project sponsored by the Ministry of International Trade and Industry of Japan. This work is supported by "Sub-Committee of Model Tests on Embedment Effect on Reactor Building" under "Committee on Seismic Verification Test" of NUPEC. The authors wish to express their gratitude for the cooperation and valuable suggestions offered by the members of Committee.